Simultaneous measurement of distance and speed using frequency-modulated continuous-wave self-mixing interferometry and all-phase fast Fourier transform

Jinyuan Yuan (袁锦源)[1], and Bin Liu (刘斌)[1, 2*]

[1] School of Physics and Optoelectronics, Xiangtan University, Xiangtan, 411105, China

[2]SECTE, University of Wollongong, Wollongong, NSW, 2522, Australia

*Corresponding author: liubin@xtu.edu.cn

Received Month X, XXXX; accepted Month X, XXXX; posted online Month X, XXXX

In this work, we propose a method using frequency modulated continuous waveform (FMCW) laser self-mixing interferometry (SMI) and all-phase fast Fourier transform (APFFT) for simultaneous measurement of speed and distance. APFFT offers superior accuracy in frequency determination by mitigating issues like the fence effect and spectrum leakage, contributing to high-accuracy measurement for speed and distance. Both simulations and experiments have demonstrated relative errors at the level of 10^{-4} and 10^{-3} for distance and speed measurements respectively. Furthermore, factors impacting measurement performance have been discussed. It provides a high-performance and cost-effective solution for distance and speed measurements, applicable across scientific research and various industrial domains.

Keywords*: Self-mixing interferometry; FMCW interferometry; All-phase FFT; Distance and speed measurement.*
DOI: 10.3788/COLXXXXXX.XXXXXX.

1. Introduction

Achieving precise and simultaneous measurement of distance and speed is crucial across various sectors. There has been considerable research focus on developing efficient, accurate, and reliable techniques for measuring distance and speed. Traditional measurement techniques, such as ultrasonic and infrared sensors, often face limitations in accuracy and range, and are susceptible to environmental factors like temperature, humidity, and pollutants. Optical ranging techniques such as triangulation, time-of-flight methods, and coherent measurements are also widely utilized. However, there is often a trade-off between resolution and maximum distance achievable with these techniques [1]. Optical frequency-modulated continuous-wave (FMCW) interference is a promising optical technology because of its ability of simultaneous measurement for absolute distance and speed [2]. To date, a range of optical FMCW interferometric systems have been developed and showcased, e.g., Michelson FMCW interferometry, Mach-Zehnder FMCW interferometry, and Fabry-Perot FMCW interferometry.

In recent decades, a unique interferometric configuration called self-mixing interferometry (SMI) has attracted extensive research interests due to its advantages of compact structure, low-cost implementation and high measurement resolution. It relies on self-mixing effect, occurring when a proportion of laser is back-reflected by an external target and reenters the laser internal cavity, then mixes with the internal light, modulating the laser output power and frequency. Since the back-reflected light carries the information of the external cavity, the information can be extracted from the modulated laser output power or optical frequency [3]. The technology has a number of applications in measurement of displacement [4], distance [5], velocity [6], rotational speed [7], vibration [8], acoustic emission [9], laser parameters [10], particle [11],and biomedical signals [12].

In recent years, FMCW and SMI have been integrated for measurement of displacement [13-15], distance [16, 17], and speed [18]. In many applications, simultaneous measurement of absolute distance and speed is of significance and the feasibility to achieve this has been verified, where fast interpolated fast Fourier transform (FFT) has been applied to measuring the beat frequency [19, 20]. With the influence of noise and spectrum linkage, uncertainty may be induced when determining the beat frequency. Compared with the commonly used FFT, all-phase FFT (APFFT) can effectively suppress the errors caused by spectral leakage, and it can be used for non-cooperative targets and overcomes some problems generated by scattering patterns, demonstrating a good ranging resolution trade-off compared to other optical methods, and it has been used for distance measurement [17]. Therefore, in this work, FMCW SMI and APFFT are combined for simultaneous measurement of distance and speed, providing a high-performance, cost-effective solution for speed and distance measurements in scientific research and industrial applications.

2. Measurement Principle

2.1 FMCW self-mixing interferometry

In SMI-based applications, the measured laser output power, also called SMI signal, is modulated by $G(\phi)$, where $G[\cdot]$ is a periodic function of the optical phase ϕ with the expression:

$$\phi=\frac{4\pi n\nu s}{c}, \tag{1}$$

where n is the refractive index, c is the light speed in vacuum, ν is the laser optical frequency and s is the absolute distance between the laser front facet and target. When ν and s are variables with time, time differentiation of the optical phase leads to the following equation:

$$\frac{\partial \phi}{\partial t} = \frac{4\pi n}{c} \cdot \frac{\partial \nu}{\partial t} \cdot s + \frac{4\pi n}{c} \nu \cdot \frac{\partial s}{\partial t}. \quad (2)$$

Laser diode (LD) is often used as the laser source in SMI-based applications for its merits of low cost and capability of easy frequency modulation via injection current. The laser optical frequency ν is linearly modulated when applying a periodic triangular injection current to an LD within certain range. In this work, we consider the condition that the FMCW SMI system operates in weak feedback regime. Thus, the fringe frequency in the rising and falling edge of the triangular wave can be expressed as in Eqs. (3) and (4) considering $n \approx 1$ in the air.

$$f_{edge+} = \frac{1}{2\pi} \cdot \frac{\partial \phi}{\partial t} = \frac{4\Omega \Delta I}{cT_m} s + \frac{2}{\lambda_0} V, \quad (3)$$

$$f_{edge-} = \frac{1}{2\pi} \cdot \frac{\partial \phi}{\partial t} = \frac{4\Omega \Delta I}{cT_m} s - \frac{2}{\lambda_0} V, \quad (4)$$

where Ω is the optical frequency modulation efficiency with the unit GHz/mA; T_m is the modulation period; ΔI is the variation of the injection current and λ_0 is central laser wavelength during a modulation period; V is the speed of the target to be measured. Hence, according to Eqs. (3) and (4), the distance s and target speed V can be obtained as:

$$s = \frac{T_m c (f_{edge+} + f_{edge-})}{8\Omega \Delta I}, \quad (5)$$

$$V = \frac{\lambda_0}{4} (f_{edge+} - f_{edge-}). \quad (6)$$

As a result, the precision of the retrieved fringe frequency in the rising and falling edge of the triangular wave determines the measurement performance of an FMCW-SMI sensing system.

2.2 All-phase fast Fourier transform

In the traditional FFT algorithm, spectral leakage resulting from the fence effect presents a computational resolution challenge. Despite efforts to mitigate this issue through methods such as spectral refinement and the energy ratio method, challenges persist. The introduction of APFFT seeks to overcome these obstacles by revolutionizing traditional spectrum analysis methods. This includes modifying input data truncation and leveraging signal phase invariance. In APFFT, data from 2N-1 points are employed for convolution, windowing, and FFT calculation to precisely derive phase and frequency information. Moreover, by employing the phase difference method with data from 3N-1 points, phase data from both the initial 2N-1 points and the final 2N-1 points are calculated independently to obtain relative phase insights. This methodology facilitates the calculation of the frequency correction value, as illustrated in Fig. 1.

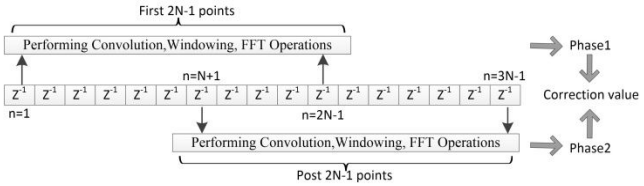

Fig.1. APFFT time-shifted phase difference (N=6)

In SMI signals, the phase remains independent of the frequency offset, simplifying the estimation of amplitude, frequency, and phase based on the phase difference facilitated by APFFT. This method, compared to traditional spectral analysis techniques, effectively reduces spectral leakage and improves precision. As a result, it allows for the extraction of more accurate frequency information with minimal signal distortion, thereby enhancing the accuracy of distance and speed measurements. The derivation starts with a simple complex exponential signal outlined in Eq. (7), where f represents the discrete frequency and ϕ_0 denotes the initial phase.

$$d_1(n) = e^{j\left(\frac{2\pi n f}{N} + \phi_0\right)}. \quad (7)$$

Applying the general FFT with rectangular window to Eq. (7), the spectrum is expressed as follows:

$$F(k) = \frac{\sin[\pi(f-k)]}{\sin[\pi(f-k)/N]} e^{j[\phi_0 + \frac{N-1}{N}\pi(f-k)]}. \quad (8)$$

The phase extraction is primarily reliant on the accurate alignment of discrete frequencies with integer values. However, deviations from integer values pose a challenge, as truncating data with period delay exacerbates spectral leakage due to signal discontinuity, especially with non-integer frequencies. To address this, APFFT with a rectangular window is employed, yielding the depicted spectrum. Both discrete linear and circular displacement characteristics are considered in the Fourier Transform. Notably, whether aligns with an integer or not, its extraction from the APFFT spectrum remains feasible. This assertion is corroborated by the spectrum derived from Eqs. (8) and (9).

$$F_{ap}(k) = \frac{\sin^2[\pi(f-k)]}{\sin^2[\pi(f-k)/N]} \cdot e^{j\phi_0}. \quad (9)$$

The M-point delay signal of $d_1(n)$ is shown as below:

$$d_2(n) = e^{j[\frac{2\pi f}{N}(n+M)+\phi_0]}. \quad (10)$$

The specific frequency can be expressed as Eq. 11, i.e., where k^* is the main frequency, corresponding to the main peak in the frequency domain, which can be easily obtained from the major frequency peaks of $d_1(n)$ and $d_2(n)$. Δk is the decimal fraction with the value ranging from -0.5 to +0.5.

$$f = k^* + \Delta k. \quad (11)$$

Then, we denote the phases after applying APFFT on $d_1(n)$ and $d_2(n)$ by $\phi_1'(k^*)$ and $\phi_2'(k^*)$ respectively. As their values fall into the range of $\pm\pi$, and their difference must fall into the range of $\pm 2\pi$, the value of Δk can be obtained from Eq. (12) [17].

$$\Delta k = \begin{cases} \frac{1}{2\pi}\left[\phi_2'(k^*)-\phi_1'(k^*)\right]+1, & -2\pi < \phi_2'(k^*)-\phi_1'(k^*) < -\pi \\ \frac{1}{2\pi}\left[\phi_2'(k^*)-\phi_1'(k^*)\right], & -\pi \le \phi_2'(k^*)-\phi_1'(k^*) \le \pi \\ \frac{1}{2\pi}\left[\phi_2'(k^*)-\phi_1'(k^*)\right]-1, & \pi < \phi_2'(k^*)-\phi_1'(k^*) < 2\pi. \end{cases} \quad (12)$$

Finally, the final estimated frequency f_{est} is as [17]:

$$f_{est} = \frac{F_s}{N} f = \frac{F_s}{N}\left(k^* + \Delta k\right), \quad (13)$$

where F_s denotes the sampling frequency rate. Note that we typically choose $M \le N$ to reduce the effect caused by phase blurring.

2.3 Measurement performance test

Measurement performance of the APFFT algorithm has been tested and compared with the single point correction FFT method in [20] by using the simulated FMCW SMI signals. Figure 2 shows the relative errors of APFFT and single point correction FFT in speed and distance measurement. For each point, ten times of measurement has been performed and the average relative errors are calculated and shown. It can be seen that APFFT algorithm contributes less errors in both speed and distance measurement. Especially, it shows much better measurement performance than the single point correction FFT algorithm for speed measurement.

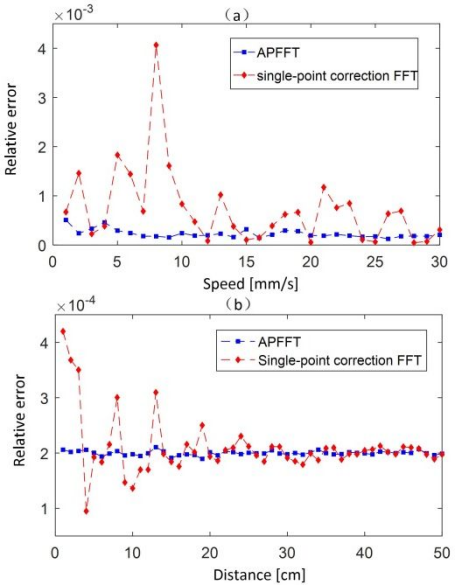

Fig. 2. Relative errors with APFFT and single-point correction FFT for (a) speed, (b) distance measurement

3. Experiment and Results

3.1 Experiment Setting

Experiments were performed using the system as depicted in Fig.3. The target to be measured is assembled on a linear stage (Thorlabs, NRT100/M). A single mode LD (Hitachi, HL8325G) with output power of 40 mW is used as the laser source which is driven by a combined LD current and temperature controller (Thorlabs, ITC4001). The attenuator is used to adjust the feedback strength to keep the system in weak feedback regime. The photodiode (PD) integrated inside the LD package works together with a customized detection circuit to convert the optical SMI signals into electrical ones and then captured by a data acquisition card. Finally, SMI signals are processed using APFFT in a PC to retrieve the distance and speed information.

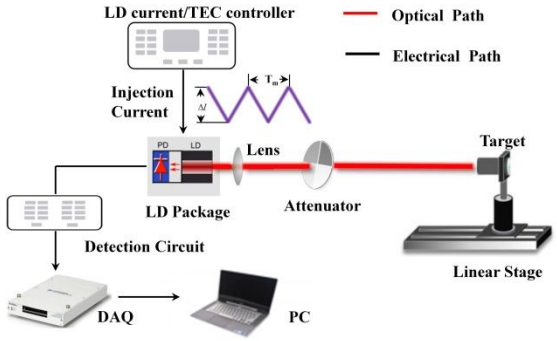

Fig. 3 Experimental setup

During the experiments, the temperature of the laser was stabilized at $T = 25 \pm 0.01\,^{\circ}C$. A periodical triangular modulated injection current with the range from 67.5 mA to 72.5 mA was applied to the LD with the built-in modulation function provided by the LD controller. The optical frequency modulation efficiency of the LD was measured with $\Omega = 2.5$ GHz/mA. The central laser wavelength is with $\lambda_0 = 836$ nm. The sampling frequency is 25 MHz. The linear stage has a maximum movement range of 100 mm, a maximum speed of 30 mm/s and an accuracy of 1 μm. Figure 4 shows a typical FMCW SMI signal. In order to facilitate the APFFT algorithm, the linear modulation triangular waveform was removed. Here, Fig. 5 is an example of the laser intensity before and after removing the triangular waveform.

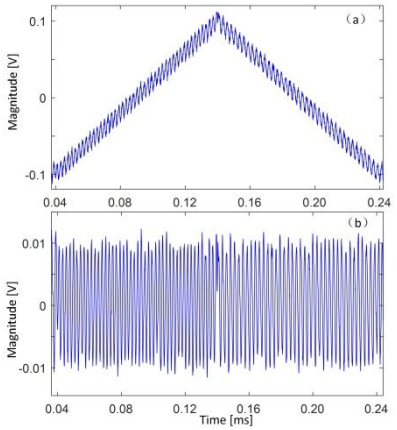

Fig. 4 (a) Example of FMCW SMI signal within one period (b) signal after removing the triangular modulation waveform.

3.2 Measurement Results

First, distance measurement has been verified. The linear stage was put 100 cm away from the LD. Then, we use the software to control the stage to specific positions. Figure 5 shows the measurement results of the distance from 100 cm to 110 cm. It can be found that the measurement results show good accuracy and relative error is at the scale of 10^{-4} Figure 6 depicts the measurement results when the linear stage moves with different speeds, which demonstrates good accuracy with the relative error at the scale of 10^{-3} . For each point, we measured ten times and took the average as the final results.

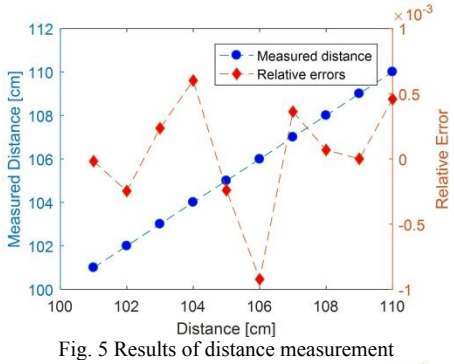

Fig. 5 Results of distance measurement

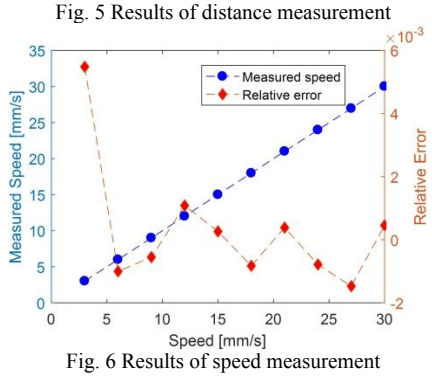

Fig. 6 Results of speed measurement

Then, dynamic movements have been applied to the target to demonstrate the feasibility of simultaneous measuring distance and speed. The first one is a linear movement achieved by the linear stage, and the speed was set with 30 mm/s. Figure 7 shows the measurement results and relative errors. The other one is a sinusoidal movement which was applied by a piezo transducer (PI, P-810.20).The transducer was put 50 cm away from the laser and a sinusoidal movement was applied with an amplitude of 10 μm and frequency of 400 Hz. The measured results are presented in Fig.8.

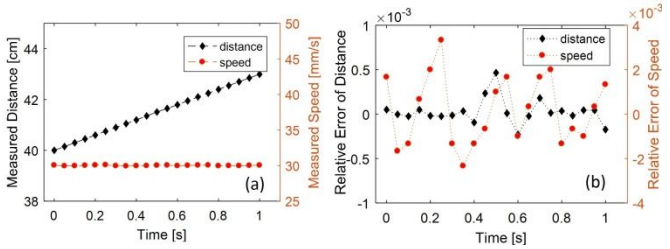

Fig. 7 Results of simultaneous distance and speed measurement for linear movement

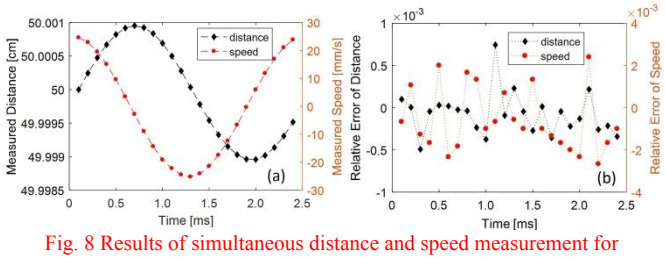

Fig. 8 Results of simultaneous distance and speed measurement for sinusoidal movement

From above results, it can be seen that the proposed method of FMCW SMI with combination of APFFT algorithm is able to achieve simultaneous measurement of distance and speed with high accuracy and the merits of SMI technology like compact structure and low-cost implementation.

4. Discussion

In an SMI system, the laser frequency changes due to optical feedback effect, which is determined by a parameter named optical feedback factor C . The value of C characterizes the operation regime of an SMI system, i.e., the system is at weak feedback regime when $C<1$ and it is at moderate/strong regime when $C\geq 1$. The effect of the optical feedback can be neglected when $C=1$. Thus, the weak feedback regime with $C=1$ was selected to maintain the accuracy of the APFFT results in this work. In order to fulfill the requirement, the reflected optical power should be less than 0.1% of the laser output power [21], i.e, less than 0.04 mW for the laser in this work. Then, we have also calculated the optical feedback factor with $C\approx 0.3$.

Based on Eqs. (5) and (6), it can be found some other parameters can also influence the measurement performance except for the accuracy of the APFFT results. Given the accuracy of the APFFT is Δf . The accuracy of the measured distance and speed is as below:

$$\Delta s=(T_m c\Delta f)/(8\Omega\Delta I), \tag{14}$$

$$\Delta V=\lambda\Delta f/4. \tag{15}$$

It is evident that several factors influence the measurement accuracy, including the optical frequency modulation efficiency Ω , the injection current modulation period T_m , the modulation amplitude ΔI , and the initial laser wavelength λ_0 . While the optical frequency modulation efficiency is an inherent parameter of an LD, which remains fixed for a given LD, opting for an LD with a larger Ω can potentially enhance accuracy. Moreover, smaller injection current modulation periods and larger modulation amplitudes tend to improve accuracy. However, it's worth noting that larger modulation amplitudes may induce mode hopping in an LD, thereby affecting the linear relationship between injection current and laser frequency. The relationship between the injection current and laser frequency has been tested, which shows good linearity between 67 mA and 73 mA. Thus, an injection current ranging from 67.5 mA to 72.5 mA

was applied. Additionally, the initial laser wavelength also plays a crucial role in measurement performance and may shift with operational temperature variations. To address this, temperature stabilization was ensured using the LD temperature controller throughout the experiments. For FFT-based distance measurement by FMCW method, the resolution can be expressed as $c/2\Delta\nu$ where $\Delta\nu$ is the sweep bandwidth of the FMCW source and it is 12.5 GHz in this work. However, For APFFT method, it can be improved and determined by the decimal fraction in Eq. (13) with $\Delta kc/2\Delta\nu$. Thus, a micrometer-level distance resolution can be easily achieved.

The speckle effect represents another crucial factor influencing the measurement outcomes of SMI technology, particularly noticeable when the target possesses a diffusive surface or undergoes large-range movements, resulting in amplitude modulation of the SMI fringes. Despite the presence of amplitude modulation in the SMI fringes due to the speckle effect, our findings indicate minimal impact on the determined frequency through the APFFT method. Therefore, for the purposes of this study, we opted to overlook the speckle effect.

5. Conclusion

A method combining FMCW SMI with APFFT is proposed to realize simultaneous measurement of speed and distance. Compared to traditional interpolated Fourier transform methods, APFFT offers superior accuracy in frequency information by mitigating issues like the fence effect and spectrum leakage. Through both simulation and experimental validation, the method achieves relative errors at the level of 10^{-4} and 10^{-3} for distance and speed measurements respectively. Additionally, factors influencing measurement performance are discussed. Overall, this technique presents a high-performance and cost-effective solution for distance and speed measurements, suitable for applications in scientific research and industrial settings.

ACKNOWLEDGEMENTS

This study was supported by National Natural Science Foundation of China (62005234) and China Scholarship Council Post-Doctoral Program (202107230002).

References

1. G. Berkovic and E. Shafir, "Optical methods for distance and displacement measurements," Advances in Optics and Photonics **4,** 441 (2012).
2. J. Zheng, "Single-Mode Birefringent Fiber Frequency-Modulated Continuous- Wave Interferometric Strain Sensor," IEEE Sensors Journal **10,** 281 (2010).
3. X. Wang, L. Feng, P. Chen, Z. Huang, and Y. Yuan, "Micro displacement reconstruction of self-mixing grating interferometer based on Littrow structure," Chinese Optics Letters **19,** 101402 (2021).
4. Z. Huang, X. Hu, Q. Li, X. Jin, B. Xu, D. Wang, X. Liu, T. Zhang, Z. Zhang, G. Chen, C. Li, and D. Li, "Phase-Shifted Quadrature-Phase demodulation based on a Multi-Longitudinal mode laser Self-Mixing sensor for displacement measurement," Measurement **206,** 112323 (2023).
5. Y. Zhao, C. Wang, Y. Zhao, D. Zhu, and L. Lu, "An All-Fiber Self-Mixing Range Finder With Tunable Fiber Ring Cavity Laser Source," J Lightwave Technol **39,** 4217 (2021).
6. D. Guo, H. Jiang, L. Shi, and M. Wang, "Laser self-mixing grating interferometer for MEMS accelerometer testing," IEEE Photonics Journal **10,** 1 (2018).
7. C. Jiang, Y. Geng, Y. Liu, Y. Liu, P. Chen, and S. Yin, "Rotation velocity measurement based on self-mixing interference with a dual-external-cavity single-laser diode," Applid Optics **58,** 604 (2019).
8. S. Ge, Y. Lin, H. Chen, X. Kong, D. Zhu, Z. Dong, X. Wang, and W. Huang, "Signal extraction method based on spectral processing for a dual-channel SMI vibration sensor," Optics and Lasers in Engineering **164,** 107531 (2023).
9. B. Liu, Y. Ruan, and Y. Yu, "All-Fiber Laser-Self-Mixing Sensor for Acoustic Emission Measurement," Journal of Lightwave Technology **39,** 4062 (2021).
10. L. An and B. Liu, "Measuring parameters of laser self-mixing interferometry sensor based on back propagation neural network," Optics Express **30,** 19134 (2022).
11. Y. Zhao, J. Li, M. Zhang, Y. Zhao, J. Zou, and T. Chen, "Phase-unwrapping algorithm combined with wavelet transform and Hilbert transform in self-mixing interference for individual microscale particle detection," Chinese Optics Letters **21,** 041204 (2023).
12. H. Liang, Y. Wang, L. Kan, K. Xu, T. Dong, W. Wang, B. Gao, and C. Jiang, "Wearable and Multifunctional Self-Mixing Microfiber Sensor for Human Health Monitoring," IEEE Sensors Journal **23,** 2122 (2023).
13. D. Guo and M. Wang, "Self-mixing interferometer based on temporal-carrier phase-shifting technique for micro-displacement reconstruction," Opt Commun **263,** 91 (2006).
14. Q. Gong, "Study on the Micro-displacement Measuring System by Laser Self-mixing Effect," (National University of Defense Technology, Changsha, China, 2016).
15. A. Jha, F. J. Azcona, and S. Royo, "Frequency-Modulated Optical Feedback Interferometry for Nanometric Scale Vibrometry," IEEE Photonics Technology Letters **28,** 1217 (2016).
16. K. Kou, X. Li, L. Li, H. Li, and T. Wu, "Absolute distance estimation with improved genetic algorithm in laser self-mixing scheme," Optics & Laser Technology **68,** 113 (2015).
17. K. Kou, C. Wang, and Y. Liu, "All-phase FFT based distance measurement in laser self-mixing interferometry," Optics and Lasers in Engineering **142,** 106611 (2021).
18. Y. Zhao, D. Zhu, Y. Chen, Y. Tu, T. Bi, Y. Zhao, B. Yu, and L. Lu, "All-fiber self-mixing laser Doppler velocimetry with much less than 0.1 pW optical feedback based on adjustable gain," Optics Letters **45,** 3565 (2020).
19. Y. Wang, Z. Hua, J. Shi, Z. Dai, J. Wang, L. Shao, and Y. Tan, "Laser Feedback Frequency-Modulated Continuous-Wave LiDAR and 3-D Imaging," IEEE Transactions on Instrumenation and Measurement **72,** 7002309, (2023).
20. M. Norgia, D. Melchionni, and A. Pesatori, "Self-mixing instrument for simultaneous distance and speed measurement," Optics and Lasers in Engineering **99,** 31 (2017).
21. J. Ohtsubo, *Semiconductor lasers: stability, instability and chaos* (Springer, 2012).